

# Intracellular mechanisms regulating apoB-containing lipoprotein assembly and secretion in primary hamster hepatocytes

Changiz Taghibiglou, Debbie Rudy, Stephen C. Van Iderstine, Andrea Aiton, Dora Cavallo, Raphael Cheung, and Khosrow Adeli<sup>1</sup>

Division of Clinical Biochemistry, Department of Laboratory Medicine and Pathobiology, Hospital for Sick Children, University of Toronto, Toronto, Ontario, Canada M5G 1X8

**Abstract** We studied the biogenesis of apolipoprotein B (apoB) in primary hepatocytes isolated from hamster liver, an animal model with striking resemblance to humans in lipoprotein metabolism. Hamster hepatocytes were found to assemble and secrete apoB-containing lipoproteins at a density of VLDL. Intracellular mechanisms of apoB biogenesis were investigated in both intact and permeabilized hamster hepatocytes. Translocational status of hamster apoB-100 was examined using trypsin protection assays in permeabilized cells as well as isolated microsomes which revealed that 27–42% of newly synthesized apoB was trypsin accessible as opposed to a control protein, transferrin, which was found to be essentially insensitive to exogenous trypsin. Subcellular fractionation of membrane and luminal apoB pools indicated, however, that only a minor fraction of hamster apoB was associated with the microsomal membrane. Approximately 40% of newly synthesized apoB was found to be degraded post-translationally in a process sensitive to MG132. Immunoblotting analysis of apoB immunoprecipitates revealed ubiquitination of hamster apoB suggesting the involvement of the proteasome in its intracellular turnover. In addition to MG132, *o*-phenanthroline, a metalloprotease inhibitor, was also effective in stabilizing hamster apoB. Experiments in permeabilized hamster hepatocytes further confirmed post-translational instability of hamster apoB which was degraded over a 3-h chase generating proteolytic fragments including 167, 70, 57, and 46 kDa intermediates. Of these only the 70 kDa fragment was ALLN sensitive. Oleate treatment of hamster hepatocytes provided protection against intracellular apoB degradation, but did not stimulate its extracellular secretion. ApoB was assembled in the microsomal lumen into lipoprotein particles with densities of LDL and VLDL which were subsequently secreted as VLDL with a minor fraction forming HDL-like particles. In summary, hamster hepatocytes appear to efficiently assemble and secrete apoB-containing VLDL, although a significant pool of newly synthesized apoB is retained intracellularly and becomes sensitive to proteasome-mediated degradation as well as other proteases in the secretory pathway, generating specific degradative intermediates.—Taghibiglou, C., D. Rudy, S. C. Van Iderstine, A. Aiton, D. Cavallo, R. Cheung, and K. Adeli. Intracellular mechanisms regulating apoB-containing lipoprotein assembly and secretion in primary hamster hepatocytes. *J. Lipid Res.* 2000. 41: 499–513.

**Supplementary key words** Syrian golden hamster • liver • lipoprotein • VLDL • synthesis • degradation • translocation

The Syrian golden hamster has been used with increasing frequency in recent years to study hepatic lipid metabolism (1–3). The hamster has attracted increasing attention as a model for lipoprotein research because its lipoprotein metabolism appears to more closely resemble that in humans (4–6). In contrast to HepG2 cells, hamster liver produces apolipoprotein B (apoB)-containing lipoproteins with a density close to that of human VLDL (6), which functions as the main plasma cholesterol carrier in this species (7, 8). Despite the obvious advantages of this animal model in studying lipoprotein metabolism, little is known about the intracellular biogenesis and assembly of hamster apoB-100-containing lipoproteins.

ApoB-100, the major protein in VLDL and the only protein in LDL, is a large hydrophobic protein of 4536 amino acids with a molecular mass of approximately 550 kDa. Hepatic apoB mRNA level is relatively stable and generally does not change under conditions that alter its extracellular secretion (9–11). This has focused attention on co- and post-translational mechanisms that modulate hepatic apoB secretion. Of particular interest has been the transit of apoB in the secretory pathway and its translocation

Abbreviations: ALLN, N-acetyl-leucyl-leucyl-norleucinal; apoB, apolipoprotein B; CSK, cytoskeletal buffer; ER, endoplasmic reticulum; EST (2S,3S0-trans-epoxysuccinyl-1-leucylamido-3-methyl-butane ethyl ester); HDL, high density lipoproteins; LDL, low density lipoproteins; MEM, minimum essential medium; MTP, microsomal triglyceride transfer protein; PAGE, polyacrylamide gel electrophoresis; PMSF, phenylmethylsulfonyl fluoride; SDS, sodium dodecyl sulfate; VLDL, very low density lipoproteins

<sup>1</sup> To whom correspondence should be addressed.

across the ER membrane. Although there is consensus that apoB becomes associated with the inner leaflet of the ER membrane, there is controversy concerning whether apoB develops a transmembrane orientation in the ER at some point during its transit in the secretory pathway. As a secretory protein, apoB contains a signal peptide, is N-linked glycosylated, and does not possess a classic transmembrane spanning domain (12). Thus the formation of a transmembrane pool of apoB presents a biological paradox. However, several lines of evidence support the notion that apoB becomes transmembrane after arrest of its translocation across the ER membrane (13–15). Evidence was provided for the formation of translocationally arrested apoB in HepG2 cells, with a 69-kD NH<sub>2</sub> terminus domain residing in the lumen of microsomes, and the remaining domains of apoB being exposed on the cytoplasmic surface of the ER membrane (15). Cytosolic exposure of newly synthesized apoB has also been demonstrated in a number of other studies using isolated microsomes (16–23). Studies in permeabilized HepG2 cells have also suggested that a significant pool of newly synthesized apoB is susceptible to exogenous trypsin (24), further supporting the data from isolated microsomes. Finally, a recent study used protease protection assays and immunocytochemistry to argue that apoB, although most probably largely translocated into the lumen of the ER during translation, does assume a transmembrane orientation in the ER membrane of permeabilized HepG2 cells (25).

In contrast, there is also evidence that argues against a transmembrane orientation for apoB. Shelness, Morris-Rogers, and Ingram (26) used COS-1 cells transfected with human apoB-50 and showed a complete luminal localization of apoB. Furthermore, protease-protection assays of membrane vesicles isolated from HepG2 cells demonstrated that a majority of endogenous apoB was protected from exogenous protease (27, 28). In vitro translation experiments with apoB-30 mRNA in the presence of dog pancreas microsomes also failed to demonstrate an exposed cytosolic orientation for apoB (29).

In HepG2 cells, approximately one half to two thirds of de novo synthesized apoB is degraded (30–32). In primary cell cultures of rat hepatocytes (33–35), 25% to 50% of the newly synthesized apoB appears to be degraded whereas the extent of degradation is about 44–50% in primary rabbit hepatocytes (36, 37). ApoB degradation was initially thought to occur in a pre-Golgi compartment (17, 30–32), in a process inhibited by ALLN (30, 38, 39), mostly based on evidence from HepG2 cells. More recently, several reports have appeared on the role of the ubiquitin–proteasome system in apoB degradation (40–42). Newly synthesized apoB appears to be subject to rapid co-translational degradation by the cytosolic proteasome (40–42). Benoist and Grand-Perret (43), using a microsomal triglyceride transfer protein (MTP) inhibitor, showed that apoB could undergo co-translational degradation by the proteasome when MTP activity was reduced. In a recent report, Chen, LeCaherec, and Chuck (42) detected ubiquitin–apoB that was associated with the Sec61 complex and showed that factors including calnexin, which

alter translocation, can affect apoB ubiquitination and degradation. ApoB degradation may also occur post-translocationally and even after an apoB-lipoprotein particle is formed. Although there are some differences in the major site of intracellular degradation of apoB among various hepatoma cell lines and primary hepatocytes, overall results indicate that apoB degradation can occur at multiple sites in the secretory pathway by a variety of as yet unidentified or partially identified proteases (for recent reviews refer to 44, 45).

Although a great deal of information on apoB biogenesis and VLDL metabolism has been obtained in rat, chicken, and rabbit hepatocytes, or cell lines such as HepG2 and McArdle 7777 cells, there are limitations to using these cell models to study the regulation of VLDL synthesis and secretion in humans. Notably, rat liver secretes both apoB-48 and apoB-100, whereas human and hamster livers secrete only apoB-100. Although rabbit liver secretes only apoB-100, its cholesterol metabolism is different from that of humans. In addition, while HepG2 cells secrete only apoB-100, it is in the form of LDL/HDL particles rather than normal VLDL. In the present study, we have investigated the intracellular mechanisms regulating apoB biosynthesis, degradation, lipoprotein assembly, and secretion in primary hamster hepatocytes, a primary cell model exclusively expressing apoB-100-containing VLDL particles.

## EXPERIMENTAL PROCEDURES

Male Syrian golden hamsters (*Mesocricetus auratus*) were purchased from Charles River (Montreal, PQ). Fetal bovine serum, liver perfusion, wash, digest, and attachment media were obtained from Life Technologies (Grand Island, NY). Drugs used for animal surgery were ketamine hydrochloride from Vetrepharm Canada (London, ON), xylazine from Bayer (Etobicoke, ON), lidocaine from Langford (Guelph, ON), and acepromazine from Ayerst Laboratories (Montreal, PQ). All surgical disposable materials were obtained from Ethicon (Somerville, NJ) or Johnson & Johnson Medical Inc. (Arlington, TX). Oleic acid, 360  $\mu$ m, complexed to albumin (oleate/BSA ratio of 8:1) was prepared as described (46). Rabbit anti-rat transferrin (which cross-reacts with hamster transferrin) was purchased from Cappell (West Chester, PA). Rabbit anti-hamster apoB antiserum was prepared commercially by Lampire Biological Laboratories (Pipersville, PA) using hamster LDL prepared in our laboratory. Specificity of this commercial preparation of anti-apoB polyclonal antibody and lack of any cross-reactivity to other hamster apolipoproteins (apoA-I or apoE) was confirmed by immunoblotting analysis of purified plasma lipoprotein fractions.

### Isolation of primary hamster hepatocytes

Male Syrian golden hamsters weighing between 100–120 g were sedated and anesthetized by an intramuscular injection of acepromazine (1 mg/kg) and intraperitoneal injection of a mixture of ketamine (200 mg/kg) and xylazine (10 mg/kg). Liver was perfused as described (47) with several modifications which included using commercial liver perfusion and liver digest media to achieve partial liver tissue digestion. The animal was placed on a heating pad to reduce loss of body heat and an incision was made along the abdomen exposing the liver and intestines. A 2-

gauge butterfly needle was inserted into the abdominal vena cava and sutured in place such that flow to the kidneys was arrested. The liver was isolated from the circulatory system by two further sutures, one blocking the thoracic aorta and caudal vena cava and one below the insertion point of the needle blocking the abdominal aorta and abdominal vena cava. Once the sutures had been tied, the portal vena was cut and perfusion by a peristaltic pump (Pharmacia Biotech) began at a rate of 3.6 mL/min. Solutions used in perfusion were heated to 39°C and filtered through a 0.22- $\mu$ m syringe filter. They were also aerated with 100% oxygen and supplemented with penicillin G and streptomycin as well as 10 mm HEPES, pH 7.2, to prevent pH drift. Initial perfusion was with Liver Perfusion Medium (Life Technologies) until no blood was observed exiting the portal vena (~30 mL). The liver was then partially digested in situ with Liver Digest Medium (Life Technologies) delivered at 2.6 mL/min. Perfusion was stopped when liver integrity began to deteriorate as evidenced by the appearance of cracks when the tissue was gently probed (~20–25 mL of digest medium). At this point the liver was dissected out of the animal, minced with scissors, and filtered through sterile gauze using Hepatocyte Wash Medium (Life Technologies). Hepatocytes were separated by sequential centrifugations in a 50-mL conical centrifuge tube at 720, 300, 115, and 30 *g* for 5 min. After each spin, pelleted cells were resuspended in 25 mL of fresh wash medium. After the final spin hepatocytes were resuspended in 25 mL of Hamster Attachment Medium (Life Technologies) supplemented with 5% fetal bovine serum and 1  $\mu$ g/mL insulin. Cells were placed in an incubator (37°C, 5% CO<sub>2</sub>, 95% air, 100% humidity) for 30 min. Cell viability was measured by exclusion of 0.2% trypan blue and 35-mm dishes, previously coated with collagen Type I (100  $\mu$ g/dish, ICN), were seeded with 1.5 million viable cells. Cell viability varied between 60 and 75%. Dishes were incubated for 4 h to allow attachment of viable cells. Nonviable cells were removed by 2  $\times$  1 mL washes with Attachment Medium + 5% fetal bovine serum + 0.0015  $\mu$ g/mL insulin. Primary hamster hepatocytes were used in experiments either at this point or after overnight incubation and additional washing.

The viability and functional specificity of primary hepatocytes were examined by trypan blue exclusion assay, protein synthesis rate, SDS-PAGE analysis of cell extracts and the synthesis and secretion of hepatic specific proteins, albumin and apoB. We consistently obtained a 60–75% cell viability ( $67.5 \pm 6.5\%$ , in four representative animals) based on trypan blue exclusion assay. The average yield of cellular protein recovered was also reproducible in various primary cell cultures ( $0.44 \pm 0.08$  mg protein per  $10^6$  cells,  $n = 8$ ). SDS-PAGE analysis of cell extracts and media from cultured hepatocytes indicated a consistent profile of cellular proteins over a 3-day period (data not shown). Primary hamster hepatocytes were found to maintain their synthesis and secretion of albumin for a period of at least 3 days. Densitometric analysis of the SDS-PAGE profile of media from cultured hamster hepatocytes indicated a consistent rate of albumin secretion (day 1,  $123,991 \pm 9,780$ , day 2,  $114,470 \pm 4,197$ , and day 3,  $102,452 \pm 4,327$  scan units). We also examined the ability of cultured hepatocytes to synthesize total as well as liver specific proteins after radiolabeling of primary hepatocytes isolated from various animals with [<sup>35</sup>S]methionine. Primary hepatocytes were consistently capable of incorporating [<sup>35</sup>S]methionine into TCA-precipitable protein indicating a high degree of viability ( $1,376,000 \pm 314,100$  cpm/ $10^6$  cells/h;  $n = 12$ ). Furthermore, all viable cultures were found to be capable of synthesizing and secreting liver specific proteins, apoB and albumin. The rate of albumin secretion in three different cultures of primary hepatocytes was  $34,151 \pm 1,753$  cpm/ $10^6$  cells/h, respectively.

### Metabolic labeling of intact primary hamster hepatocytes

Primary hamster hepatocytes were preincubated in methionine-free minimum essential medium (MEM) at 37°C for 1 h and pulsed with 75–100  $\mu$ Ci/ml of [<sup>35</sup>S]methionine for 45–60 min. After the pulse, the cells were washed twice and chased in hepatocyte attachment media supplemented with 10 mm methionine. At various chase times duplicate or triplicate dishes were harvested, and cells were lysed in solubilization buffer (PBS containing 1% Nonidet P-40, 1% deoxycholate, 5 mm EDTA, 1 mm EGTA, 2 mm PMSF, 0.1 mm leupeptin, 2  $\mu$ g/ml ALLN). The lysates were centrifuged for 10 min at 4°C in a microcentrifuge, and supernatants were collected for immunoprecipitation.

### Permeabilization of primary hamster hepatocytes

Primary hamster hepatocytes were permeabilized essentially as described for HepG2 cells (30). At various intervals, duplicate or triplicate dishes were washed with cytoskeletal (CSK) buffer, and solubilized in the solubilization buffer. Cell extracts were centrifuged in a microcentrifuge at 14,000 rpm, 4°C, for 10 min, and the supernatant was subjected to immunoprecipitation.

### Trypsin digestion of permeabilized primary hamster hepatocytes

Primary hamster hepatocytes were pulsed for 1 h, the radioactivity was chased for 10 min, and the cells were then permeabilized and subjected to trypsin digestion as described previously for HepG2 cells (24, 30). In some experiments, MG132 (25  $\mu$ M) was added 15 min before the pulse and was present throughout the pulse and chase.

### Isolation and trypsin treatment of hepatic microsomes

Hamster hepatocytes were pulsed for 1 h in the presence and absence of MG132 (25  $\mu$ M), and were used to prepare a microsomal fraction as described (13, 32) with minor modifications. Briefly, cells were washed and homogenized after the pulse to isolate crude microsomes. Microsomes were purified on a step gradient using two sucrose densities (1.3 m and 2.25 m) and centrifuged for 1 h at 4°C and 40,000 rpm. Microsomes collected from the interface between sucrose layers were pooled, aliquoted, and incubated  $\pm$  100  $\mu$ g/ml trypsin for 30 min at room temperature. After the incubation, soybean trypsin inhibitor (1 mg/ml) and PMSF (final concentration 100  $\mu$ M) were added and the microsomes were solubilized and subjected to immunoprecipitation.

### Isolation and subcellular fractionation of hamster liver microsomes

Isolation of the microsomal fraction and the separation of the luminal and membrane components by carbonate extraction and sucrose gradient ultracentrifugation were performed as described (16, 48–50). Intact cells were pulsed for 1 h in the presence and absence of the protease inhibitor, MG132 (25  $\mu$ M) and were then scraped in 0.5 ml of 50 mm sucrose solution supplemented with a cocktail of protease inhibitors (1 mm PMSF, 100 KIU/ml Trasylol, 1  $\mu$ M pepstatin A, and 5  $\mu$ M ALLN) and homogenized with a glass dounce homogenizer. The homogenate was centrifuged for 10 min at 2200 *g*. The supernatant containing the crude microsomes was then treated with sodium carbonate, pH 11. The luminal component released by carbonate extraction was isolated from the membrane fraction by ultracentrifugation at 37,000 rpm for 90 min at 12°C in SW41 rotor. The isolated microsomal membrane was resuspended in 1 ml of PBS, solubilized in 800  $\mu$ l of a solubilization buffer containing 360  $\mu$ l 5  $\times$  C buffer (250 mm Tris-HCl, pH 7.4, 750 mm NaCl, 25 mm EDTA, 5 mm PMSF, 5% TritonX-100), and 410  $\mu$ l PBS (containing 450 KIU/ml Trasylol, and 5 mm PMSF), and then subjected to immunoprecipitation. The luminal fractions were either directly solubilized and



immunoprecipitated for apoB, or were subjected to lipoprotein fractionation by sucrose gradient ultracentrifugation.

### Sucrose gradient fractionation of apoB-containing lipoproteins

ApoB-containing lipoproteins present in luminal contents of microsomes (prepared as above) or secreted into the medium were analyzed by gradient ultracentrifugation. The sucrose gradient was formed by layering from the bottom of the tube: 1.5 ml of 49% sucrose, 3.0 ml of 25% sucrose, 2.0 ml of 20% sucrose, 3.0 ml of sample in 12.5% sucrose, 1.9 ml of 5% sucrose, 0.9 ml of 0% sucrose. All solutions contained 1 mM phenylmethylsulfonyl fluoride, 100 kallekrein inhibitory units/ml aprotinin, 5  $\mu$ M ALLN, and 3 mM imidazole, pH 7.4. The gradient was ultracentrifuged at 35,000 rpm in a Sorval TH-641 rotor for 65 h at 12°C, unloaded into 12 fractions, and apoB was recovered from each fraction by immunoprecipitation and SDS-PAGE and fluorography. The band corresponding to apoB was cut out of the gel and digested and the radioactivity counted.

### Detection of ubiquitinated apoB by immunoblotting

Primary hamster hepatocytes were treated with 40  $\mu$ g/ml ALLN or 25  $\mu$ M MG132 for 1 h and then washed once with PBS and solubilized in the solubilizing buffer containing 5 mM *n*-ethyl maleimide (NEM). Cell lysates were immunoprecipitated for hamster apoB and then immunoblotted for ubiquitin, essentially as described (51).

### Immunoprecipitation, SDS-PAGE, and fluorography

Lysates and media were immunoprecipitated as described (30). Immunoprecipitates were washed three times and analyzed by SDS-PAGE essentially as described (52). The gels were fixed, stained, and then fluorographed by incubating in Enhance (DuPont) or Amplify (Amersham Corp.). The gels were dried and exposed to X-ray film at -80°C. To determine the radioactivity associated with apoB and its fragments, the corresponding bands were visualized by fluorography, excised from the gel, digested, and quantitated by liquid scintillation counting.

## RESULTS

### Primary hamster hepatocytes secrete apoB-containing lipoprotein at the density of VLDL

The density of apoB-containing lipoproteins secreted by hamster hepatocytes was investigated by density fractionation of isolated lipoproteins in media of cultured hamster hepatocytes labeled with [<sup>35</sup>S]methionine. In this study, after a 1-h pulse, cells were chased for 1 and 2 h in the presence and absence of ALLN (40  $\mu$ g/ml). Density of the media samples was adjusted to 1.006 g/ml. After ultracentrifugation, the top fraction (1/10 of total volume of the media) was collected and subjected to immunoprecipitation. Cell lysates were also immunoprecipitated for apoB. After a 1-h chase, 39% of total apoB was recovered in the VLDL fraction of the media; whereas after a 2-h chase, 56% of total apoB was recovered from the VLDL fraction of the media. In ALLN-treated cells, at 1 h and 2 h chase, 33% and 42% of total apoB was recovered from media VLDL, respectively. Thus ALLN treatment did not increase the efficiency of VLDL secretion (as estimated by comparing the percentage of total radiolabeled apoB secreted as VLDL-apoB). However, total radiolabeled apoB

recovered in ALLN-treated cells was about 40% higher at 0 time and more than 2-fold higher after 1 and 2 h chase times compared to control cells. Increased recovery of labeled apoB in the presence of ALLN suggested protection against co- and/or post-translational degradation of the protein during pulse and chase periods.

### Analysis of apoB translocational status in permeabilized primary hamster hepatocytes

As our preliminary studies had suggested that hamster apoB may be subject to intracellular degradation, we investigated the translocational status of hamster apoB in primary hamster hepatocytes. Translocational status of newly synthesized hamster apoB-100 was assessed based on trypsin digestion of permeabilized hamster hepatocytes. This protocol has previously been used by our laboratory to investigate apoB translocation in HepG2 cells (24) and McRH7777 cells (51). The procedure for permeabilizing primary hamster hepatocytes was similar to that previously described for HepG2 cells. Optimization experiments showed that incubation with CSK buffer containing 50  $\mu$ g/ml digitonin for 10 min or 75  $\mu$ g/ml digitonin for 5 min at room temperature was sufficient to permeabilize hamster hepatocytes without causing significant damage to intracellular organelles (as assessed by the loss of ER-luminal proteins). To confirm the integrity of intracellular membranes after the permeabilization process, we monitored the retention of radiolabeled apoB and transferrin in permeabilized cells and any possible leakage into the surrounding medium (CSK buffer). No apoB or transferrin could be recovered by immunoprecipitation from the CSK buffer (pooled solutions of CSK-digitonin and wash buffers). In addition, no significant difference was detectable in the immunoprecipitable apoB and transferrin recovered from permeabilized cells at different concentrations of digitonin. Immunoprecipitable transferrin recovered at 0, 50, and 100  $\mu$ g/ml digitonin was 11,241  $\pm$  62, 9,675  $\pm$  554, and 9,548  $\pm$  1,938 CPM/plate (*n* = 3), respectively; immunoprecipitable apoB recovered was 1,373  $\pm$  136, 1,257  $\pm$  21, and 1,284  $\pm$  43 CPM/plate (*n* = 3), respectively. The absence of labeled transferrin and apoB in the CSK buffer and the lack of a decrease in cellular levels of these proteins strongly argues against any significant leakage of newly synthesized proteins residing in the secretory pathway of permeabilized hepatocytes. This, in turn, suggests that the integrity of the ER-Golgi component of the secretory pathway remains mostly intact after permeabilization of the cells.

In this and all subsequent protease protection experiments, intact primary hamster hepatocytes were initially pulse-chased to achieve biosynthesis and translocation of apoB across the ER membrane. Permeabilization was only carried out to allow the delivery of trypsin to the cytosolic surface of the ER membrane. **Figure 1A** shows immunoprecipitable apoB recovered from permeabilized cells (pulsed for 45 min, chased for 10 min, and permeabilized) with and without trypsin digestion (in the presence or absence of Triton X-100). The amount of trypsin-resistant apoB was measured as a percentage of the intact apoB im-

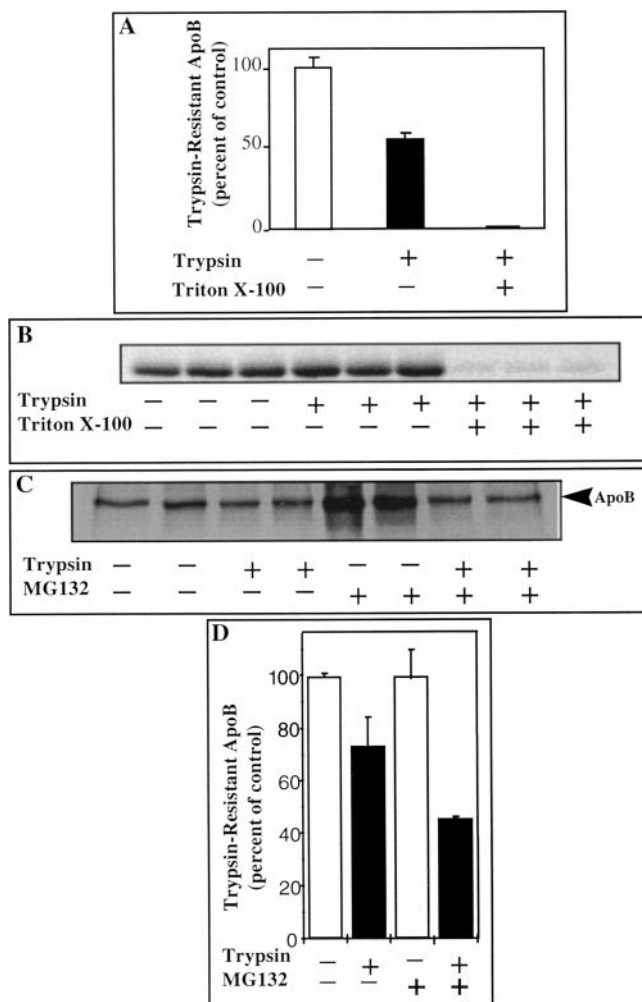


**Fig. 1.** Trypsin sensitivity of hamster apoB-100 in permeabilized hamster hepatocytes and isolated microsomes. Panel A: Primary hamster hepatocytes were pulsed with [ $^{35}\text{S}$ ]methionine for 1 h, chased in hepatocyte attachment medium plus 10 mM l-methionine for 10 min, and then incubated in CSK buffer containing 75  $\mu\text{g}/\text{ml}$  digitonin for 5 min at room temperature to achieve permeabilization. Permeabilized cells were then washed and incubated in the presence and absence of trypsin (100  $\mu\text{g}/\text{ml}$ ) or trypsin plus 0.5% Triton X-100, for 10 min at room temperature. Trypsin treatment was stopped by the addition of soybean trypsin inhibitor and other protease inhibitors. Cells were solubilized and cell extracts were subjected to immunoprecipitation by a specific anti-apoB antibody and then analyzed by SDS-PAGE and fluorography. Data shown as mean  $\pm$  SD (two separate experiments in triplicate). Panel B: protease protection experiments similar to that in panel A were performed and a control protein, transferrin, was immunoprecipitated to monitor its trypsin sensitivity in the presence and absence of Triton X-100. Panels C and D: Intact cells were pulsed for 1 h in the presence and absence of MG132 (25  $\mu\text{M}$ ) and then homogenized to isolate crude microsomes. Purified microsomes were obtained by sucrose gradient centrifugation as described in Experimental Procedures. Collected microsomes were treated with 100  $\mu\text{g}/\text{ml}$  trypsin for 30 min at room temperature. Trypsin treatment was stopped by addition of soybean trypsin inhibitor. Samples were solubilized and subjected to immunoprecipitation by a specific anti-apoB antibody and then analyzed by SDS-PAGE and fluorography. ApoB-associated radioactivity was quantitated by excision and scintillation counting of the apoB bands. C) a representative fluorograph; D) trypsin resistant apoB (mean  $\pm$  SD, three separate experiments in duplicate) as a percentage of apoB recovered in the absence of trypsin.

munoprecipitated from control cells not subjected to trypsin treatment. An average of  $42.4 \pm 10.1\%$  of newly synthesized apoB was trypsin-accessible in permeabilized cells. In the presence of both trypsin and Triton X-100, no immunoprecipitable apoB could be recovered, suggesting that the trypsin-resistant apoB detected in permeabilized cells is segregated by intracellular membranes which become accessible to trypsin upon addition of the membrane solubilizing agent, Triton X-100. Finally, percent trypsin sensitivity in permeabilized cells was significantly greater with apoB ( $42.4 \pm 10.1\%$ ) than the control protein, transferrin ( $13.9 \pm 6.2\%$ ) (Fig. 1B),  $P < 0.05$ , under similar experimental conditions. Addition of Triton X-100 to permeabilized cells caused an almost total degradation of transferrin by exogenous trypsin suggesting that transferrin was not inherently resistant to trypsin digestion (Fig. 1B).

### Trypsin sensitivity of hamster apoB-100 in isolated microsomes

Protease protection assays were also performed with microsomes isolated from hamster hepatocytes to confirm the observations made in permeabilized cells. In these experiments, hamster hepatocytes were pulse-labeled for 1 h and then used to isolate a microsomal fraction by ultracentrifugation. Isolated microsomes were then subjected to in vitro trypsin digestion. Figs. 1C and 1D indicate the amount of apoB recovered from microsomes isolated from control and MG132 (25  $\mu\text{M}$ )-treated cells in the presence and absence of exogenous trypsin. In control cells,  $27 \pm 7.9\%$  of newly synthesized microsomal apoB was trypsin accessible, whereas in MG132 treated cells,  $54.7 \pm 10.5\%$  was accessible to trypsin digestion. This difference ( $P < 0.01$ ) in trypsin sensitivity between the two conditions (nearly 2 times more in MG132-treated cells) may be attributed to the protective effect of MG132 against degradation of the pool of apoB associated with the cytosolic side of the ER membrane. It should be noted that MG132, a proteasome inhibitor, also increased the total amount of immunoprecipitated apoB 2.2-fold compared to control cells. Most of the pool protected by MG132 was thus trypsin-accessible. MG132-treated microsomes had 35% more immunoprecipitable apoB than control cells after trypsin digestion. As a control, we also examined the trypsin sensitivity of transferrin in both control and MG132-treated cells. In control cells,  $87.6 \pm 13.8\%$  ( $n = 3$ ) of labeled transferrin was resistant to trypsin digestion whereas in MG132-treated cells  $97.6 \pm 5.9\%$  ( $n = 3$ ) of labeled transferrin was trypsin resistant ( $P > 0.05$ ). Trypsin resistance of transferrin in isolated microsomes and the lack of effect of MG132 on trypsin accessibility of this control protein appear to confirm the specificity of the observations with respect to protease sensitivity of apoB in control and MG132-treated cells.

### Analysis of apoB-100 in subcellular fractions of isolated microsomes

Intracellular distribution of newly synthesized apoB-100 in primary hamster hepatocytes was examined by isolating a total microsomal fraction and preparing luminal and

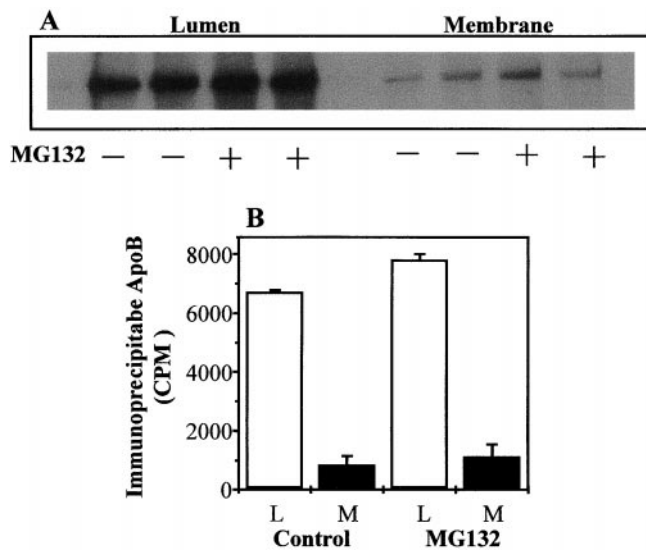


**Fig. 2.** Subcellular distribution of newly synthesized apoB in microsomal membrane and lumen. Primary hamster hepatocytes were pulsed (1 h) and chased (5 min) in the presence and absence of 25  $\mu$ M MG132. Cells were washed, homogenized, and subsequently subjected to subcellular fractionation to isolate microsomes. Luminal apoB was extracted from microsomes by carbonate treatment and separated from the membrane fraction by centrifugation (SW41 rotor, 37,000 rpm, 90 min). Both the membrane and luminal fractions were immunoprecipitated with a specific anti-apoB antibody and analyzed by SDS-PAGE and fluorography. ApoB radioactivity was quantitated by cutting and scintillation counting of the apoB band. A) representative fluorograph; B) distribution of labeled apoB in membrane (M) and lumen (L) of isolated microsomes.

membrane subfractions. **Figures 2A** and **2B** show the results of such an experiment. A small fraction of newly synthesized apoB was consistently found to be associated with microsomal membrane ( $11.2\% \pm 4.1$ ). However, a large pool of radiolabeled apoB could be extracted with sodium carbonate and was thus detected in the soluble luminal fraction of microsomes. The distribution of microsomal apoB in the luminal and membrane pools did not change with MG132 pretreatment of the cells (control cells,  $88.8\% \pm 0.7$  luminal apoB, and  $11.2\% \pm 4.1$  membrane apoB; MG132-treated cells,  $86.5\% \pm 0.9$  luminal apoB, and  $12.8\% \pm 4.5$  membrane apoB). Although the ratio of the pools was similar in control and MG132-treated cells, treatment with the inhibitor increased total and luminal apoB by  $18.5\% \pm 7.6$  and  $16.3\% \pm 2.6$ , respectively. Similar observations were made when subcellular fractionation studies were performed in the presence of ALLN as the protease inhibitor. ALLN treatment did not alter the proportion of newly synthesized apoB found associated with the membrane and luminal fractions of microsomes. After a 1-h pulse in control cells,  $80.7\%$  and  $19.3\%$  of immunoprecipitated apoB was luminal and membrane-bound, respectively, whereas in ALLN-treated cells,  $83.2\%$  and  $16.8\%$  of apoB was recovered in lumen and membrane fractions, respectively. After a 30-min chase,  $65.3\%$ ,  $11.9\%$ , and  $22.8\%$  of immunoprecipitated apoB in control

cells, and  $67.6\%$ ,  $14.8\%$ , and  $17.6\%$  of apoB in ALLN-treated cells were recovered in lumen, membrane, and media of hamster hepatocytes, respectively. It should be noted that total immunoprecipitable apoB increased in ALLN-treated cells by  $11.1\%$  and  $19.9\%$  at 0 and 30 min chase times, respectively, compared to control cells. Furthermore, after the 30-min chase there was no significant difference in secreted apoB between control and ALLN-treated cells, but luminal and membrane-associated apoB both showed an increase of  $24\%$  and  $49\%$ , respectively, in the presence of ALLN (compared to control).

#### ApoB stability and secretion in primary hamster hepatocytes

Pulse-chase labeling experiments were performed to analyze the stability and secretion of apoB in primary hamster hepatocytes. **Figure 3A** shows the turnover of newly synthesized apoB in the presence and absence of MG132. MG132 induced accumulation of apoB during the pulse (**Fig. 3B**) and appeared to protect apoB during the chase. The kinetics of apoB degradation were further examined in a 6-h chase experiment (**Figs. 3C** and **3D**). In control cells, the percentage of cellular apoB remaining after 30, 60, 120, 240, and 360 min chase was  $72.6\% \pm 18$  ( $n = 2$ ),  $55.4\% \pm 9.3$  ( $n = 5$ ),  $25.8\% \pm 8.3$  ( $n = 7$ ),  $15.6\% \pm 1.9$  ( $n = 2$ ), and  $11.2\% \pm 1.5$  ( $n = 2$ ), respectively. The percentage of radiolabeled apoB secreted into the media at the same time points was  $12\% \pm 1.4$ ,  $31\% \pm 5$ ,  $35.3\% \pm 2.1$ ,  $36\% \pm 2.9$ , and  $40.3\% \pm 7.9$ , respectively. Percent apoB degraded after a 30-min chase was  $15.8\% \pm 14$  which increased to  $38.8\% \pm 6.2$  and  $48.3\% \pm 0.7$  after 120 and 240 min chase, respectively. Interestingly, after a 4-h chase, degradation reached a plateau ( $48.4\% \pm 6.6$ ) and no further degradation occurred after a 6-h chase.

Treatment with MG132 significantly altered the pattern of apoB degradation kinetics. In these experiments, cells were treated with MG132 15 min before the pulse, and then chased in the presence of the protease inhibitor. As depicted in **Fig. 3D**, the percentage of cellular apoB remaining decreased during the chase from 100% at 0 time to  $99.4\% \pm 26$  ( $n = 2$ ),  $77.2\% \pm 8.5$  ( $n = 5$ ),  $61.2\% \pm 10$  ( $n = 7$ ),  $32\% \pm 2.2$  ( $n = 2$ ), and  $25.1\% \pm 2.7$  ( $n = 2$ ) at 30, 60, 120, 240, and 360 min chase time, respectively. Due to protection of apoB from degradation, the percentage of cellular apoB remaining in MG132-treated cells was significantly higher than the control at various time points. Interestingly, the percentage of radiolabeled apoB secreted into the media of the above cells showed no significant difference between MG132-treated and control cells. In MG132-treated cells, at 30, 60, 120, 240, and 360 min chase points,  $10.4\% \pm 1$ ,  $22.3\% \pm 2.9$ ,  $36\% \pm 4.6$ ,  $35.5\% \pm 3.3$ , and  $42.4\% \pm 2$  of radiolabeled apoB was secreted into the media, respectively. ApoB was stabilized considerably with MG132 treatment. In fact, no significant degradation occurred for the initial 2 h of chase (average of  $0.5\%$  at 60 and  $2.7\%$  at 120 min), but it was dramatically increased to  $34.8\% \pm 6.3$  at 240 min and remained approximately constant up to the end of the chase period ( $33\% \pm 6.6$  at 360 min).



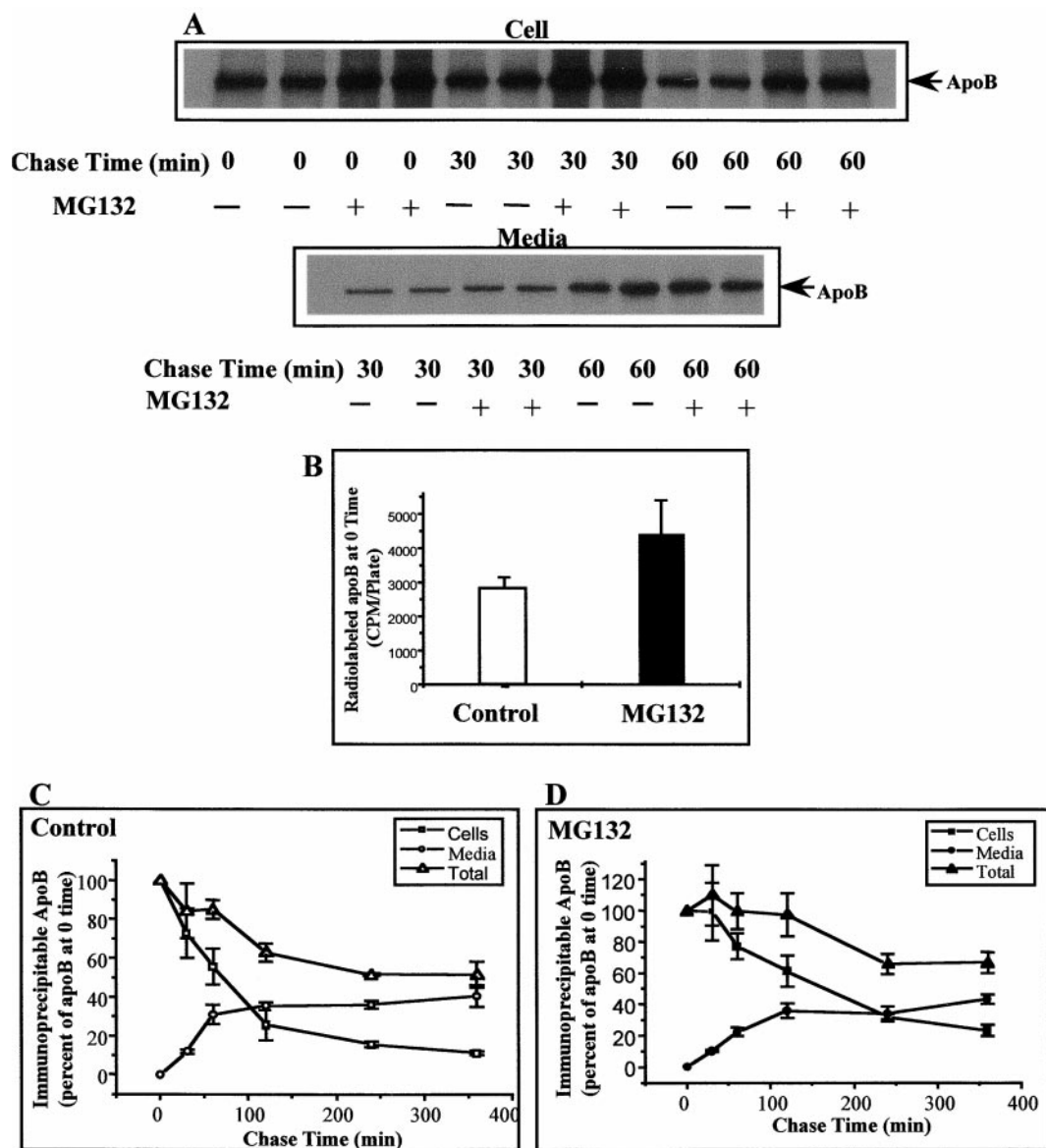


**Fig. 3.** ApoB stability and secretion in control and MG132-treated intact primary hamster hepatocytes. Primary hamster hepatocytes were pulsed with [<sup>35</sup>S]methionine and chased for up to 6 h. MG132 (25  $\mu$ M) was added 15 min before the pulse and was present throughout. Media samples and cell lysates were collected at each chase time point, subjected to immunoprecipitation, and then analyzed by SDS-PAGE and fluorography. Panel A shows a representative experiment in control and MG132-treated cells (five separate pulse-chase labeling experiments were performed with similar results). Panel B shows the effect of MG132 on apoB accumulation during the pulse (at 0 time) (mean  $\pm$  SD of the pulse-chase experiment in panel A). Panels C and D show the results of several experiments at 0, 30, 60, 120, 240, and 360 min chase times. Panel C shows the distribution of apoB in cells (open squares), media (open circles) as well as the total apoB (open triangles) in control hamster hepatocytes expressed as a percent of labeled apoB at 0 time. Panel D shows the percentage of apoB in cells (closed squares), media (closed circles) as well as the total apoB (closed triangle) in MG132-treated cells. Data shown as mean  $\pm$  SD of a representative pulse-chase experiment performed in triplicate.

#### ApoB degradation in permeabilized primary hamster hepatocytes and detection of degradation intermediates

Experiments were also performed in permeabilized hamster hepatocytes. Cells were pulsed and then permeabilized and chased in CSK buffer for different time points from 0 to 180 min in the presence and absence of ALLN. **Figure 4A** shows the pattern of apoB degradation in permeabilized hamster hepatocytes. ApoB was gradually degraded in permeabilized cells such that the percentage of apoB remaining was  $91.6\% \pm 15.2$  (n = 2),  $91.6\% \pm$

$6.3$  (n = 4),  $76.3\% \pm 2.4$  (n = 2),  $77.6\% \pm 2.4$  (n = 4), and  $51.9\% \pm 4.9$  (n = 4) at 30, 60, 90, 120, and 180 min chase times, respectively. Degradation was more prominent after 60 min chase and reached  $48.1\% \pm 4.9$  (n = 4) after 180 min chase. The extent of degradation in permeabilized cells was lower than that observed in intact cells during the first 2 h chase ( $8.2\% \pm 6.3$  and  $22.4\% \pm 2.5$  in permeabilized cells compared with  $17.8\% \pm 8$  and  $38.8\% \pm 6.2$  in intact cells at 60 and 120 min chase, respectively). Interestingly, several degradation fragments were observed

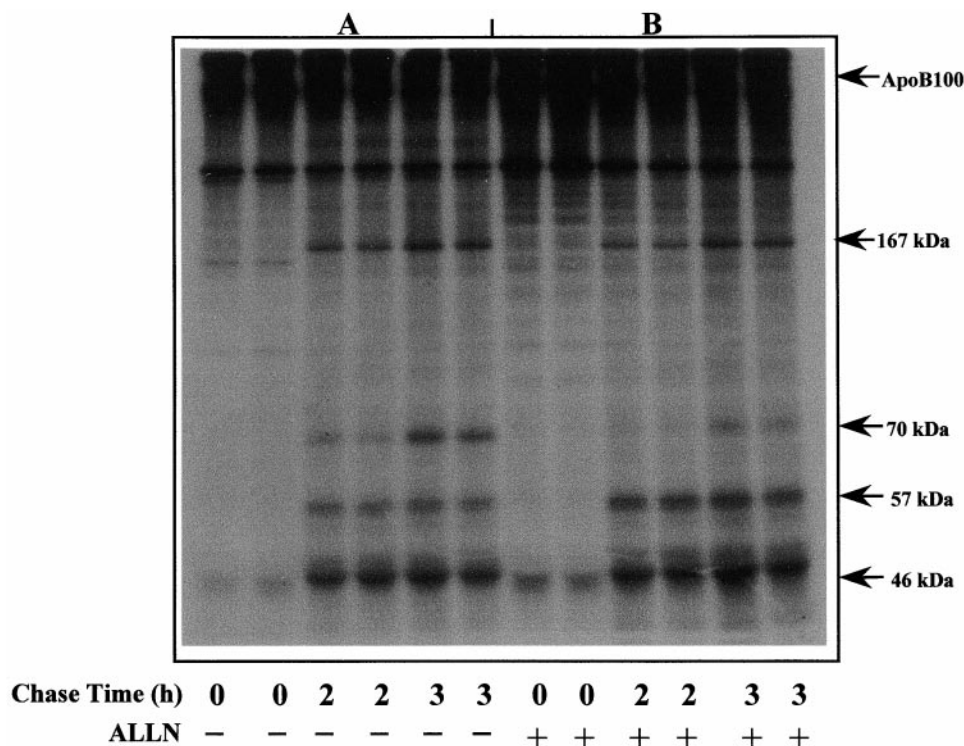


**Fig. 4.** Intracellular stability of apoB in permeabilized primary hamster hepatocytes. Primary hamster hepatocytes were pulsed with [<sup>35</sup>S]methionine and then permeabilized with 50  $\mu$ g/ml digitonin in CSK buffer for 10 min at room temperature. Permeabilized cells were incubated in CSK buffer for 0, 2, and 3 h. ALLN (40  $\mu$ g/ml) was added 15 min before the pulse and was present throughout the experiment. Cells were solubilized and cell extracts were subjected to immunoprecipitation with a specific anti-apoB antibody and then analyzed by SDS-PAGE and fluorography. The position of the intact apoB-100 and its degradation fragments (167, 70, 57, and 46 kDa) are indicated with arrowheads. A) control cells; B) ALLN-treated cells.

in permeabilized cells with approximate molecular masses of 167, 70, 57, and 46 kDa. The 70 kDa fragment was surprisingly identical to the fragment previously observed in HepG2 cells (30, 53). This is the first report of the appearance of a 70 kDa apoB fragment in primary hamster hepatocytes. Also shown in Fig. 4B is the effect of ALLN on apoB degradation in permeabilized cells. Interestingly, the appearance of the 70 kDa fragment was ALLN-sensitive and was almost entirely abolished in ALLN-treated permeabilized cells. ALLN caused a significant protection against degradation in permeabilized cells especially at 120 and 180 min chase times (percent apoB-100 remaining was  $94.8\% \pm 2.2$  and  $78.8\% \pm 0.1$ , respectively). MG132 showed a similar protective effect on apoB-100 degradation although it did not inhibit the generation of the 70 kDa fragment (data not shown). The formation of the 46, 57, and 167 kDa fragments were both ALLN- and MG132-insensitive.

#### The sensitivity of apoB degradation to various protease inhibitors

To more extensively characterize apoB degradation in hamster hepatocytes, the effect of a number of protease inhibitors, including ALLN (40  $\mu$ g/ml), lactacystin (2.5  $\mu$ M), EST (40  $\mu$ g/ml), PMSF (1 mM), leupeptin (100  $\mu$ g/ml), and *o*-phenanthroline (200  $\mu$ g/ml), on cellular and

secreted apoB was determined after a 2-h pulse. The results, shown in Fig. 5, are expressed as immunoprecipitable apoB recovered/total labeled protein under control and various experimental conditions. Among various protease inhibitors tested, only *o*-phenanthroline had statistically significant ( $P < 0.05$ ) effects on total apoB remaining in cells + media. Both ALLN and lactacystin appeared to increase cellular apoB but did not significantly affect total apoB remaining. In contrast treatment with *o*-phenanthroline, a metalloprotease inhibitor, significantly increased both cellular and secreted apoB, and thus enhanced total apoB remaining, indicating a considerable effect of this metalloprotease inhibitor on apoB accumulation.

#### Ubiquitin-proteasome pathway is involved in hamster apoB degradation

Inhibition of hamster apoB turnover by MG132 appeared to implicate the ubiquitin-proteasome system in the degradation process. To further investigate the involvement of the proteasome, hamster hepatocytes pretreated with ALLN (40  $\mu$ g/ml) or MG132 (25  $\mu$ M) were solubilized and the cell lysates were immunoprecipitated with anti-apoB antibody and then immunoblotted with anti-ubiquitin antibodies. As shown in Fig. 6, immunoblotting of immunoprecipitated apoB by an anti-ubiquitin antibody revealed a specific and consistent pattern of polyubiquitinated apoB.



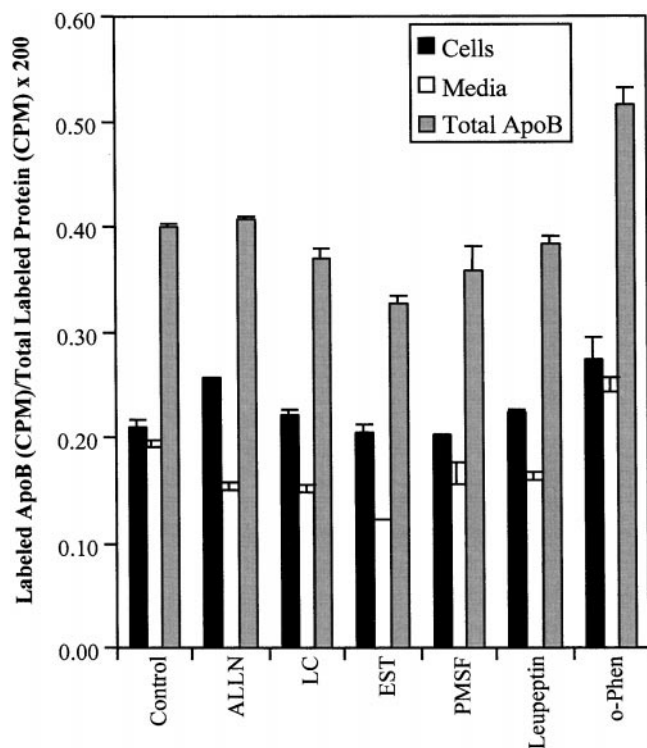


**Fig. 5.** Effect of various protease inhibitors on apoB stability and secretion. Primary hamster hepatocytes were pulsed with 100  $\mu$ Ci/ml [ $^{35}$ S]methionine for 2 h, in the presence and absence of different protease inhibitors including ALLN (40  $\mu$ g/ml), lactacystin (2.5  $\mu$ M), EST (40  $\mu$ g/ml), PMSF (1 mM), leupeptin (0.1 mg/ml), and *o*-phenanthroline (200  $\mu$ g/ml). Cell lysates and media were collected and subjected to immunoprecipitation with a specific anti-apoB antibody. Immunoprecipitates were analyzed by SDS-PAGE and fluorography as described under Experimental Procedures. The apoB band was excised and associated radioactivity was measured by scintillation counting. Cellular (black bars), media (gray bars), and total apoB (white bars) are expressed as apoB radioactivity normalized against total TCA-precipitable radioactivity in each dish (mean  $\pm$  SD,  $n = 3$ ).

In the absence of any inhibitor, only a small amount of ubiquitinated apoB could be detected, most likely as a result of rapid proteasomal degradation. There was a considerable increase in ubiquitinated apoB upon pretreatment of the cells with either ALLN or MG132 (Fig. 6). Overall these data support the notion that hamster apoB undergoes ubiquitination and is targeted for degradation by the proteasome.

#### Assembly and secretion of hamster apoB-100 VLDL

In order to investigate the assembly and secretion of apoB-containing lipoproteins in primary hamster hepatocytes, cells were labeled with [ $^{35}$ S]methionine, chased for 0 or 1 h, and used to isolate microsomes. Luminal content of microsomes as well as culture media at each chase time were subjected to sucrose gradient ultracentrifugation as described in the methods section. Fractions 1 through 5 represent high density apoB lipoprotein particles (apoB lipoproteins with a density similar to that of HDL, peak density 1.065 to 1.170 g/ml), fractions 6–10 represent the lower density apoB lipoprotein particles

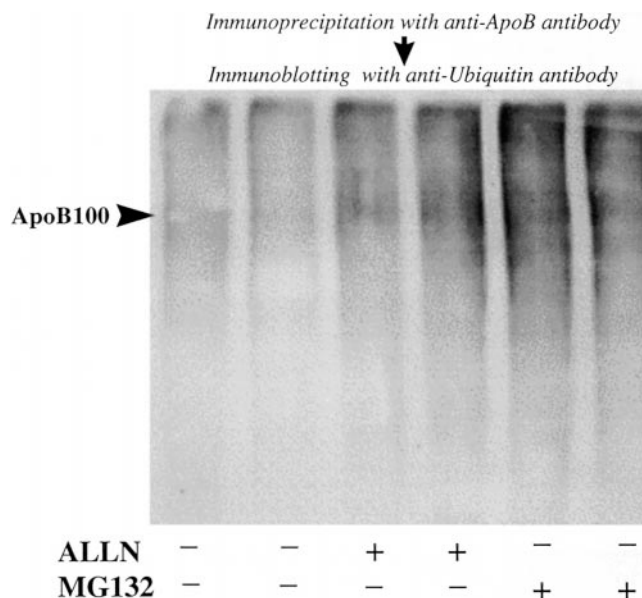


**Fig. 6.** Evidence for ubiquitination of hamster apoB-100 in primary hamster hepatocytes. Primary hamster hepatocytes ( $4 \times 35$  mm dishes) were pretreated with proteasome inhibitors, ALLN, or MG132 for 1 h, washed, solubilized, and cell lysates were first immunoprecipitated for hamster apoB and the apoB immunoprecipitates were subjected to SDS-PAGE using 4.5% polyacrylamide mini-gels. After SDS-PAGE, the proteins were transferred electrophoretically onto nitrocellulose membranes, and the membranes were immunoblotted with an anti-ubiquitin primary antibody, followed by detection using a secondary antibody conjugated to peroxidase and an ECL detection reagent. Lanes 1–2, control cells, lanes 3–4, ALLN-treated cells, lanes 5–6, MG132-treated cells. The figure shown is representative of two independent experiments.

(LDL-apoB, peak density 1.011 to 1.045 g/ml) and the top fractions, 11 and 12, contain very low density apoB lipoprotein particles (density < 1.011) (see references 16, 54). Results depicted in Fig. 7A indicate that in the microsomal lumen, radiolabeled apoB was distributed in three different density regions of the gradient with the majority of newly synthesized apoB being present in the low density fractions. There was a small pool of labeled apoB associated with the dense fractions at time 0 which increased after a 1-h chase. The luminal apoB lipoproteins in the low density as well as the very low density fractions of the gradient both decreased after a 1-h chase. Sucrose gradient ultracentrifugation of media samples revealed that the secreted form of apoB lipoprotein particles was present only in the very low density fractions of the gradient (fractions 11 and 12). Very low density lipoprotein particles were present at 0 time in the media but were increased significantly after a 1-h chase (Fig. 7B, fractions 10–12). Secretion of apoB-VLDL particles appeared to coincide with their disappearance from the luminal top light fraction.

In this study the distribution of membrane-associated apoB was also assessed by immunoprecipitating apoB from the membrane pellet recovered during subcellular fractionation of luminal contents and membrane fractions. The results are shown in Fig. 7C. Membrane bound apoB remaining at 1 h chase was 58.5% of that at 0 time. It

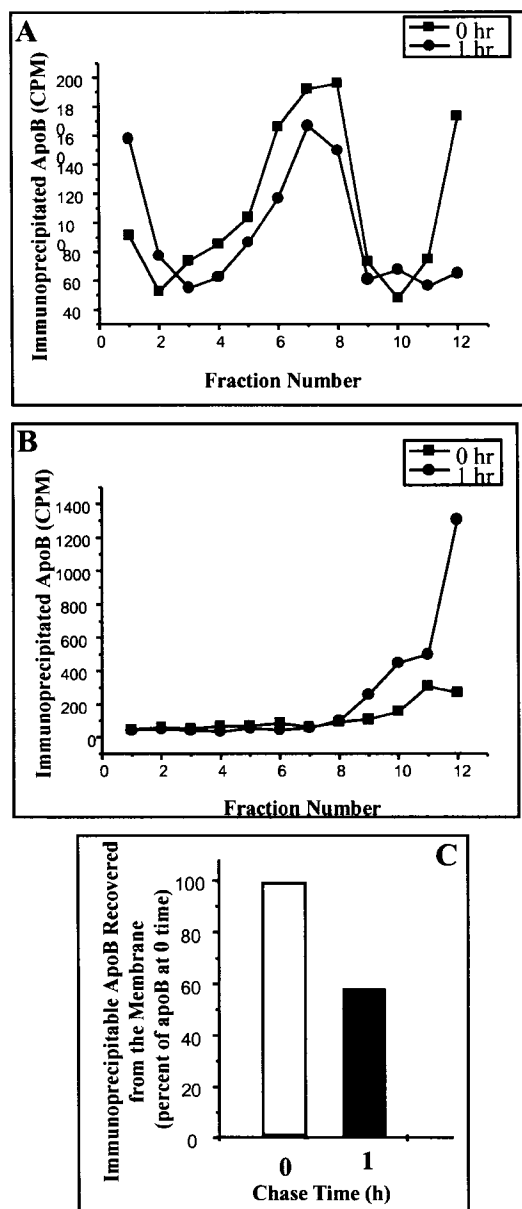


**Fig. 7.** Analysis of apoB-100-containing lipoproteins in microsomal fractions of primary hamster hepatocytes. Primary hamster hepatocytes were pulsed, chased for 0 and 1 h, and used to prepare a total microsomal fraction. Luminal contents of isolated microsomes as well as culture media were subjected to ultracentrifugation in a sucrose gradient. The gradient was fractionated from the bottom into 12 fractions, and apoB was immunoprecipitated from each fraction. Microsomal membranes were also solubilized and subjected to immunoprecipitation with a specific anti-apoB antibody. Immunoprecipitates were analyzed by SDS-PAGE and fluorography. The apoB band was excised and its radioactivity was determined by scintillation counting. Panels A and B show apoB recovered from luminal and media fractions at 0 time (closed squares) and 1 h chase (closed circles), respectively. Panel C shows membrane apoB recovered at 1 h expressed as a percentage of that present at 0 time. The figure shown is representative of two independent experiments.

appears that during the 1-h chase, 42.5% of labeled apoB disappeared from the membrane either as a result of translocation across the ER membrane and/or intracellular degradation.

### Effect of oleate on the stability and secretion of apoB in primary hamster hepatocytes

The effect of exogenous oleate on the stability and secretion of apoB was determined after an overnight pretreatment. **Figure 8** shows the immunoprecipitated apoB in cells and media, as well as total apoB remaining in control and oleate-treated hamster hepatocytes. Oleate treatment increased cellular apoB at both 1 h and 4 h chase (Fig. 8A). Despite the stabilizing effect of oleate on cellular apoB, no stimulation of apoB secretion could be observed at either 1 h or 4 h chase compared to control cells (Fig. 8B). In control cells, total apoB remaining decreased

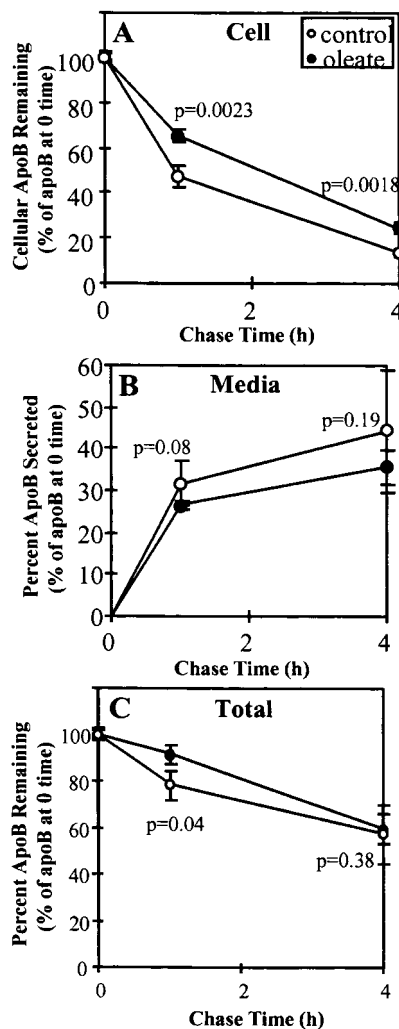


**Fig. 8.** Effect of oleate on stability and secretion of apoB in primary hamster hepatocytes. Cells were treated with hepatocyte attachment medium supplemented with either BSA or an oleate-albumin complex (oleate/BSA ratio of 8:1). After overnight incubation, both oleate-treated and control cells were pulsed with 100  $\mu\text{Ci/ml}$  [ $^{35}\text{S}$ ]methionine, and then chased in the presence (oleate-treated cells) and absence (control cells) of oleate for 0, 1, and 4 h. Cell lysates and collected media were subjected to immunoprecipitation and analyzed by SDS-PAGE and fluorography. The apoB band was cut out and counted. Panels A and B show apoB recovered from cells and media of control (open circles) and oleate-treated (closed circles) cells. In panel C, total apoB remaining (cell + media) is shown in control (open circles) and oleate-treated cells (closed circles) at different periods of chase (mean  $\pm$  SD,  $n = 6$ ).

from 100% at 0 time to  $78.4\% \pm 9.2$  and  $57.2\% \pm 12.7$  at 1 and 4 h chase times, respectively (Fig. 8C). In oleate-treated cells, total apoB remaining decreased from 100% at 0 time to  $91.5\% \pm 3.9$  and  $59.7\% \pm 6.7$  at 1 and 4 h chase periods, respectively (Fig. 8C). The protective effect of oleate against apoB degradation was thus evident after the first hour of chase but not at 4 h.

## DISCUSSION

Extensive data are currently available on mechanisms of apoB translocation and degradation, based on studies in hepatoma cell lines, such as HepG2 and McRH7777 cells, or in primary cells expressing both apoB-48 and apoB-100. In the present study, we have attempted to elucidate intracellular mechanisms of apoB biosynthesis in primary hamster hepatocytes, which synthesize and secrete apoB-100-containing VLDL particles similar to human VLDL in both size and composition. We examined translocational status of hamster apoB-100, its intracellular stability, and the process of VLDL assembly in hamster hepatocytes.

Protease protection experiments revealed that between 27 and 42% of newly synthesized apoB was trypsin-accessible depending on the methodology used. A greater sensitivity to exogenous trypsin was observed for radiolabeled apoB in permeabilized cells compared to isolated microsomes. However, this difference was not statistically significant ( $42.4 \pm 10.1\%$  in permeabilized cells vs.  $27 \pm 7.9\%$  in isolated microsomes,  $P = 0.09$ ). The trypsin accessibility of apoB in permeabilized cells or isolated microsomes was not due to non-specific perforation of microsomal membranes in these systems, based on control experiments with transferrin showing minimal trypsin sensitivity of this control protein under similar experimental conditions. One possible factor contributing to the variability observed in trypsin accessibility of hamster apoB in permeabilized cells versus isolated microsomes may be the different pulse and chase times used in these experiments and may reflect differential sensitivity of apoB to trypsin at different times during its transit in the secretory pathway. In addition, although some variability in the degree of trypsin accessibility of hamster apoB was observed in different experiments, trypsin sensitivity was still significantly higher with apoB compared to the control protein, transferrin (percent trypsin sensitivity in isolated microsomes: transferrin,  $11.3 \pm 1.6\%$ ; apoB,  $27 \pm 7.9\%$ ,  $P < 0.05$ ) (percent trypsin sensitivity in permeabilized cells: transferrin,  $13.9 \pm 6.2\%$ ; apoB,  $42.4 \pm 10.1\%$ ,  $P < 0.05$ ).

Membrane association of newly synthesized hamster apoB was also examined by carbonate extraction of isolated microsomes. Only about 11% of radiolabeled apoB was retained in the membrane fraction after carbonate extraction with the majority of labeled apoB recovered in the luminal fraction. Thus carbonate resistance of apoB did not correlate well with the percent trypsin sensitivity of apoB in protease protection experiments. However, carbonate resistance may not be a reliable reflection of translocational status of apoB as there are large differ-

ences in carbonate extractable apoB reported in various published studies (14, 50, 55). Indeed, using a revised extraction protocol, Rustaeus and colleagues (56) recently showed that most of labeled apoB could be extracted with sodium carbonate from McA-RH7777 microsomes in the form of lipoproteins. It is thus possible that some of the trypsin-accessible and membrane-associated apoB might not be necessarily resistant to carbonate extraction.

Overall our protease protection studies in both permeabilized hamster hepatocytes and isolated microsomes appear to indicate that a fraction of newly synthesized hamster apoB may be trypsin accessible, suggesting cytosolic exposure. However, as carbonate extraction studies of isolated microsomes do not support a large degree of membrane association and there was some variability in trypsin-accessible apoB in various experiments, further studies are needed to determine the nature of membrane association of hamster apoB or whether it forms a transmembrane orientation in these primary hepatocytes.

Interestingly, we observed an increased trypsin sensitivity of newly synthesized apoB in MG132-treated microsomes (nearly 2-fold), suggesting that inhibition of proteasomal degradation may cause accumulation of cytosolically exposed apoB molecules. Under these conditions, analysis of a control protein, transferrin, did not reveal any significant change in sensitivity to exogenous trypsin treatment, suggesting that the effect of MG132 was specific to apoB.

Subcellular distribution of newly synthesized apoB has been previously investigated in several primary cell types. In chick hepatocytes, approximately 50% of newly synthesized apoB was membrane associated (55). Davis et al. (13) reported that in RER isolated from rat liver, 56% of apoB-100 and 70% of apoB-48 were sensitive to exogenous trypsin, indicating that a significant amount of apoB remained on the cytosolic side of the ER membrane. Similar observations were also reported in primary rat (57), and primary chicken hepatocytes (14). Cartwright, Hebbachi, and Higgins (58) reported that in freshly isolated hepatocytes from normal and orotic acid-fed rats, 80–90% of apoB in the ER was membrane-bound. Wang, Hobman, and Brindley (21) also reported that in primary rat hepatocytes 78–85% of apoB-100 associated with the ER was in the membrane fraction.

As detailed in the introduction, there is also evidence indicating minimal sensitivity of apoB to exogenous protease during its transit in the secretory pathway, based on studies in COS-1 cells transfected with human apoB50 (26) as well as protease-protection assays of membrane vesicles isolated from HepG2 cells (27, 28). Studies in rabbit hepatocytes (59) have also shown that only about 10% of apoB becomes membrane associated. In the present study in primary hamster hepatocytes, we also found that only 11% of newly synthesized hamster apoB was associated with microsomal membrane, based on carbonate extraction of isolated microsomes. Thus, our data on carbonate resistance of apoB in hamster hepatocytes appears to compare well with rabbit hepatocytes, which also exclusively synthesize and secrete apoB-100-containing lipoproteins.

Pulse-chase labeling experiments in primary hamster



hepatocytes revealed that in intact hepatocytes nearly 40% of the labeled apoB was degraded intracellularly with less than half of the newly synthesized apoB pool secreted into the extracellular medium over a 2-h chase period. The extent of hamster apoB-100 degradation in our present study was relatively similar to that observed in primary rabbit hepatocytes (37). Intracellular degradation of hamster apoB was found to be sensitive to the proteasome inhibitor, MG132. Furthermore, immunoblotting analysis of ALLN- and MG132-treated cells with an anti-ubiquitin antibody confirmed that hamster apoB-100 is subjected to intracellular ubiquitination, further supporting a role for the ubiquitin-proteasome system in hamster apoB turnover. These observations are clearly in accord with those in established hepatoma cell lines such as HepG2 (40–42) and suggest a close similarity between apoB degradative mechanisms operating in hamster hepatocytes and HepG2 cells. Interestingly, while MG132 stabilized cellular apoB levels, no stimulation of apoB secretion was observed. Bonnardel and Davis (18) made similar observations in ALLN-treated HepG2 cells and concluded that translocation, but not degradation determines the intracellular fate of de novo synthesized apoB in these cells.

To further investigate the mechanisms of hamster apoB degradation, we permeabilized primary hamster hepatocytes. Degradation of apoB in permeabilized hamster hepatocytes coincided with the appearance of a number of apoB fragments ranging in mass from 46 to 167 kDa. Consistent detection of these fragments suggests that intact apoB may be clipped by one or more ER-associated protease(s) to yield several degradation intermediates. Interestingly, generation of the 70 kDa fragment was ALLN sensitive, while the appearance of the 46, 57, and 167 kDa fragments was insensitive to both ALLN and MG132 indicating the involvement of different proteases in the degradation of hamster apoB-100. Although some of the proteolytic fragments detected in our study may be similar to those detected previously in HepG2 cells (30, 53), this is the first report of both ALLN- and MG132-insensitive fragments in permeabilized hamster hepatocytes. We have recently provided evidence arguing that a non-proteasomal degradative pathway may be responsible for the generation of some of fragments generated in permeabilized HepG2 cells (60). Further studies are underway to determine the mechanisms by which hamster apoB fragments are generated in primary hepatocytes.

Our experiments with a variety of protease inhibitors also showed that in addition to the proteasome inhibitor, MG132, hamster apoB degradation was sensitive to *o*-phenanthroline, a metalloprotease inhibitor. These findings further suggest the involvement of other unidentified protease systems in the turnover of hamster apoB. In most other primary hepatocytes examined, degradation of apoB is not confined to the ER (61) and appears to occur even after an apoB-lipoprotein is formed (20, 21, 37, 62, 63). Cartwright and Higgins (37) found that in freshly isolated rabbit hepatocytes, inhibitors of metalloproteases (*o*-phenanthroline), serine proteases (aprotinin), serine/cysteine proteases (leupeptin) or cysteine proteases (calpain


inhibitor I; ALLN) but not aspartate proteases (pepstatin) reduced intracellular apoB degradation. Other investigators have also shown the sensitivity of apoB degradation in rat primary hepatocytes to leupeptin, a lysosomal cysteine protease inhibitor (21) and the inhibition of post-ER degradation of apoB by EST, a cysteine protease inhibitor (21). Very recently, Kendrick and Higgins (64) also showed that hamster apoB degradation is sensitive to both ALLN and *o*-phenanthroline. In our experiments, we found that ALLN inhibited fragmentation of apoB in permeabilized cells (Fig. 4) and increased the level of ubiquitinated apoB detected (Fig. 6), exhibited either no effect or an inhibitory effect on intracellular apoB accumulation depending on experimental protocol used (Fig. 5). ALLN inhibited apoB degradation in a pulse-chase labeling experiment, but did not affect the amount of total apoB remaining in cells pulsed for 2 h. These apparently conflicting results may be due to a possible inhibition of apoB synthesis when cells are pulsed for a longer period of time (2 h). Any inhibition of apoB synthesis will reduce the total apoB radioactivity remaining and will thus mask any possible effect of apoB degradation. The lack of effect of lactacystin, which is also an inhibitor of proteasome similar to MG132, on total apoB remaining in pulse-labeling experiments was also unexpected. This may be caused by either the inability of intact cells to take up and accumulate sufficient amounts of active inhibitor or the inefficiency of this inhibitor to reach the degradative compartments in intact primary hamster hepatocytes. Higher concentrations of lactacystin may be required to achieve a detectable degree of protection against intracellular degradation in intact primary cells. In contrast, MG132 may be more easily taken up by hamster hepatocytes contributing to its more potent inhibitory effect on apoB degradation. Finally, it is also important to consider that there may be differences between cells in their sensitivity to protease inhibitors with some primary hepatocytes being insensitive to certain inhibitors. Thus ALLN, which is well established as an inhibitor of proteasome-mediated degradation of apoB in HepG2 cells, has been reported to be ineffective in inhibiting apoB degradation in primary rat hepatocytes (35).

Based on evidence obtained from density gradient fractionation of luminal lipoproteins, hamster apoB-100 appears to initially assemble into LDL-like particles in the microsomal lumen. Such LDL-like particles appeared to gradually recruit more lipids forming lipid-rich VLDL particles, which were subsequently secreted into the media in the form of mature VLDL. We also found a small pool of radiolabeled apoB in the high density fraction of the lumen which increased after a 1-h chase. Based on previous observations in HepG2 cells (16), HDL-like particles may represent lipoprotein precursors which either mature by recruiting lipids forming VLDL particles, or are sorted to intracellular degradation. In freshly isolated rat hepatocytes (58), the majority of apoB in the RER and SER fractions was also found to be associated with HDL-like particles, while the apoB of VLDL density was predominantly found in *trans*- and *cis*-Golgi fractions (58). Further studies

by these investigators in primary rabbit hepatocytes appeared to support their initial observations in rat hepatocytes (59). It was thus suggested that assembly of apoB into complete VLDL is not a co-translational process and most lipids become associated with apoB late in the ER compartment and are further modified in the Golgi lumen (59). More recently, Rustaeus et al. (56) reported that in McA-RH7777 cells, membrane associated apoB-100 is partially lipidated and can be converted to VLDL. They proposed that the assembly of apoB-100-VLDL from membrane associated apoB involves an early MTP-dependent phase and a late MTP-independent phase, during which the major amount of lipid is added. It was also suggested that luminal apoB-100 in the HDL density range may be a precursor to the less dense apoB-100-containing lipoproteins. In these experiments, virtually all apoB was extractable from microsomal membranes using a revised carbonate extraction protocol (56). More recently, Wang, Tran, and Yao (65), using McA-RH7777 cells, showed that MTP is a prerequisite for the post-translational assembly of TG-enriched VLDL and it plays a role in facilitating accumulation of TG within microsomes. In conclusion, it appears that in HepG2 cells, McA-RH7777 cells, and rabbit and rat hepatocytes, a significant amount of newly synthesized apoB-100 is incorporated into a dense fraction. Our findings on VLDL assembly in primary hamster hepatocytes are partly in agreement with the observations in other primary hepatocytes (66) and established cell lines. However, hamster hepatocytes appear to form a smaller pool of HDL-like particles, although their detection suggests that the lipoprotein assembly process in these cells may be similar to that described in other hepatic model systems examined.

In contrast to HepG2 cells, treatment with exogenous oleate did not stimulate apoB secretion by primary hamster hepatocytes. Instead, oleate increased stability of cellular apoB (over the first hour of chase) without affecting its extracellular secretion. These observations compare well with a previous report on the effects of oleate on apoB secretion by hamster hepatocytes (67). Despite the lack of an effect on apoB secretion, oleate treatment appeared to enhance the stability of newly synthesized apoB molecules in hamster hepatocytes. It has been previously suggested that oleate treatment of HepG2 cells facilitates translocation of newly synthesized apoB across the ER-membrane, which in turn reduces early degradation (24). However, whether or not this protection of early degradation stimulates apoB secretion appears to differ among different cell types. In HepG2 cells, exogenous oleate significantly stimulates apoB secretion (10, 11, 50). White et al. (68) reached similar conclusions using a rat hepatoma cell line. However, Sparks et al. (69) reported an inhibitory effect of oleate on the secretion of apoB in McArdle H7777 cells and no effect on apoB secretion or cellular apoB of primary rat hepatocytes. Cartwright and Higgins (37) reported that in freshly isolated rabbit hepatocytes, oleate, in addition to prevention of cellular apoB degradation, stimulated its secretion as much as 6-fold. In contrast, no stimulatory effect of oleate on secretion of apoB was observed in rat (70, 71), hamster (67), or human

hepatocytes (72). Overall, the effect of oleate on the stability and secretion of apoB appears to be controversial. The oleate effect may depend on the cell type (primary vs. transformed cell line), turnover of the TG/fatty acid in the cells, size of cellular TG pool, and duration of incubation with oleate. In a recent report, Salter et al. (73) compared TG turnover of hamster and rat hepatocytes, and found that hamster hepatocytes had a larger intracellular TG pool and a lower rate of VLDL-TG secretion compared to rat hepatocytes. In the hamster liver, a larger proportion of newly synthesized TG was retained within the cell, rather than secreted as VLDL (compared to the rat). Overall, our finding that treatment with exogenous oleate failed to stimulate hamster apoB-100 secretion appears to correlate with data obtained in primary rat and human hepatocytes, but not those in rabbit hepatocytes.

In conclusion, the hamster appears to represent an excellent model system for further investigation of the hepatic assembly and secretion of apoB-containing lipoproteins and their hormonal and pharmaceutical modulation, without many of the drawbacks associated with the use of other primary or established cell culture model systems. The data presented in this report help to elucidate the mechanisms governing the intracellular biogenesis and extracellular secretion of hamster apoB-100, and provide the basis for future studies in this animal model system. 

This work was supported by an operating grant (NA3562) from the Heart and Stroke Foundation of Ontario to K.A.

Manuscript received 29 April 1999, in revised form 15 October 1999, and in revised form 23 December 1999.

## REFERENCES

1. Nistor, A., A. Bulla, D. A. Filip, and A. Radu. 1987. The hyperlipidemic hamster as a model of experimental atherosclerosis. *Atherosclerosis*. **68**: 159–173.
2. Kowala, M. C., J. J. Nunnari, S. K. Durham, and R. J. Nicolosi. 1991. Doxazosin and cholestyramine similarly decrease fatty streak formation in the aortic arch of hyperlipidemic hamsters. *Atherosclerosis*. **91**: 35–49.
3. Salter, A. M., E. H. Mangiapane, A. J. Bennett, J. S. Bruce, M. A. Billett, K. L. Anderton, C. B. Marenah, N. Lawson, and D. A. White. 1998. The effect of different dietary fatty acids on lipoprotein metabolism: concentration-dependent effects of diets enriched in oleic, myristic, palmitic and stearic acids. *Br. J. Nutr.* **79**: 195–202.
4. Goulinet, S., and M. J. Chapman. 1993. Plasma lipoproteins in the golden Syrian hamster (*Mesocricetus auratus*): heterogeneity of apoB- and apoA-I-containing particles. *J. Lipid Res.* **34**: 943–959.
5. Hoang, V. Q., N. J. Pearce, K. E. Suckling, and K. M. Botham. 1995. Evaluation of cultured hamster hepatocytes as an experimental model for the study of very low density lipoprotein secretion. *Biochim. Biophys. Acta*. **1254**: 37–44.
6. Liu, G. L., L. M. Fan, and R. N. Redinger. 1991. The association of hepatic apoprotein and lipid metabolism in hamsters and rats. *Comp. Biochem. Physiol.* **99**: 223–228.
7. Spady, D. K., and J. M. Dietschy. 1983. Sterol synthesis in vivo in 18 tissues of the squirrel monkey, guinea pig, rabbit, hamster, and rat. *J. Lipid Res.* **24**: 303–315.
8. Spady, D. K., J. B. Meddings, and J. M. Dietschy. 1986. Kinetic constants for receptor-dependent and receptor-independent low density lipoprotein transport in the tissues of the rat and hamster. *J. Clin. Invest.* **77**: 1474–1481.
9. Dashti, N., D. L. Williams, and P. Alaupovic. 1989. Effects of oleate

- and insulin on the production rates and cellular mRNA concentrations of apolipoproteins in HepG2 cells. *J. Lipid Res.* **30**: 1365–1373.
10. Dixon, J. L., S. Furukawa, and H. N. Ginsberg. 1991. Oleate stimulates secretion of apolipoprotein B-containing lipoproteins from HepG2 cells by inhibiting early intracellular degradation of apolipoprotein B. *J. Biol. Chem.* **266**: 5080–5086.
  11. Pullinger, C. R., J. D. North, B. B. Teng, V. A. Rifici, A. E. Ronhild de Brito, and J. Scott. 1989. The apolipoprotein B gene is constitutively expressed in HepG2 cells: regulation of secretion by oleic acid, albumin, and insulin, and measurement of the mRNA half-life. *J. Lipid Res.* **30**: 1065–1077.
  12. Knott, T. J., R. J. Pease, L. M. Powell, S. C. Wallis, S. C. Rall, Jr., T. L. Innerarity, B. Blackhart, W. H. Taylor, Y. Marcel, R. Milne, D. Johnson, M. Fuller, A. J. Lusis, B. J. McCarthy, B. Levy-Wilson, and J. Scott. 1986. Complete protein sequence and identification of structural domains of human apolipoprotein B. *Nature.* **323**: 734–738.
  13. Davis, R. A., R. N. Thrift, C. C. Wu, and K. E. Howell. 1990. Apolipoprotein B is both integrated into and translocated across the endoplasmic reticulum membrane. Evidence for two functionally distinct pools. *J. Biol. Chem.* **265**: 10005–10011.
  14. Dixon, J. L., R. Chattopadhyay, T. Huima, C. M. Redman, and D. Banerjee. 1992. Biosynthesis of lipoprotein: location of nascent apoAI and apoB in the rough endoplasmic reticulum of chicken hepatocytes. *J. Cell. Biol.* **117**: 1161–1169.
  15. Du, E. Z., J. Kurth, S. L. Wang, P. Humiston, and R. A. Davis. 1994. Proteolysis-coupled secretion of the N terminus of apolipoprotein B. Characterization of a transient, translocation arrested intermediate. *J. Biol. Chem.* **269**: 24169–24176.
  16. Boren, J., L. Graham, M. Wettsten, J. Scott, A. White, and S. O. Olofsson. 1992. The assembly and secretion of ApoB-100-containing lipoproteins in HepG2 cells. ApoB-100 is cotranslationally integrated into lipoproteins. *J. Biol. Chem.* **267**: 9858–9867.
  17. Furukawa, S., N. Sakata, H. N. Ginsberg, and J. L. Dixon. 1992. Studies of the sites of intracellular degradation of apolipoprotein B in HepG2 cells. *J. Biol. Chem.* **267**: 22630–22638.
  18. Bonnardel, J. A., and R. A. Davis. 1995. In HepG2 cells, translocation, not degradation, determines the fate of the de novo synthesized apolipoprotein B. *J. Biol. Chem.* **270**: 28892–28896.
  19. McLeod, R. S., Y. Wang, S. Wang, A. Rusinol, P. Links, and Z. Yao. 1996. Apolipoprotein B sequence requirements for hepatic very low density lipoprotein assembly. Evidence that hydrophobic sequences within apolipoprotein B48 mediate lipid recruitment. *J. Biol. Chem.* **271**: 18445–18455.
  20. Verkade, H. J., D. G. Fast, A. E. Rusinol, D. G. Scraha, and D. E. Vance. 1993. Impaired biosynthesis of phosphatidylcholine causes a decrease in the number of very low density lipoprotein particles in the Golgi but not in the endoplasmic reticulum of rat liver. *J. Biol. Chem.* **268**: 24990–24996.
  21. Wang, C. N., T. C. Hobman, and D. N. Brindley. 1995. Degradation of apolipoprotein B in cultured rat hepatocytes occurs in a post-endoplasmic reticulum compartment. *J. Biol. Chem.* **270**: 24924–24931.
  22. Wilkinson, J., J. A. Higgins, P. Groot, E. Gherardi, and D. Bowyer. 1993. Topography of apolipoprotein B in subcellular fractions of rabbit liver probed with a panel of monoclonal antibodies. *J. Lipid Res.* **34**: 815–825.
  23. Rusinol, A. E., E. Y. Chan, and J. E. Vance. 1993. Movement of apolipoprotein B into the lumen of microsomes from hepatocytes is disrupted in membranes enriched in phosphatidylmonomethyl-ethanolamine. *J. Biol. Chem.* **268**: 25168–25175.
  24. Macri, J., and K. Adeli. 1997. Studies on intracellular translocation of apolipoprotein B in a permeabilized HepG2 system. *J. Biol. Chem.* **272**: 7328–7337.
  25. Du, X., J. D. Stoops, J. R. Mertz, C. M. Stanley, and J. L. Dixon. 1998. Identification of two regions in apolipoprotein B100 that are exposed on the cytosolic side of the endoplasmic reticulum membrane. *J. Cell. Biol.* **141**: 585–599.
  26. Shelness, G. S., K. C. Morris-Rogers, and M. F. Ingram. 1994. Apolipoprotein B48-membrane interactions. Absence of transmembrane localization in nonhepatic cells. *J. Biol. Chem.* **269**: 9310–9318.
  27. Ingram, M. F., and G. S. Shelness. 1996. Apolipoprotein B-100 destined for lipoprotein assembly and intracellular degradation undergoes efficient translocation across the endoplasmic reticulum membrane. *J. Lipid Res.* **37**: 2202–2214.
  28. Leiper, J. M., G. B. Harrison, J. Bayliss, J. D. Scott, and R. J. Pease. 1996. Systematic expression of the complete coding sequence of apoB-100 does not reveal transmembrane determinants. *J. Lipid Res.* **37**: 2215–2231.
  29. Pease, R. J., J. M. Leiper, G. B. Harrison, and J. Scott. 1995. Studies on the translocation of the amino terminus of apolipoprotein B into the endoplasmic reticulum. *J. Biol. Chem.* **270**: 7261–7271.
  30. Adeli, K. 1994. Regulated intracellular degradation of apolipoprotein B in semipermeable HepG2 cells. *J. Biol. Chem.* **269**: 9166–9175.
  31. Sato, R., T. Imanaka, A. Takatsuki, and T. Takano. 1990. Degradation of newly synthesized apolipoprotein B-100 in a pre-Golgi compartment. *J. Biol. Chem.* **265**: 11880–11884.
  32. Borchardt, R. A., and R. A. Davis. 1987. Intrahepatic assembly of very low density lipoproteins. Rate of transport out of the endoplasmic reticulum determines rate of secretion. *J. Biol. Chem.* **262**: 16394–16402.
  33. Martin-Sanz, P., J. E. Vance, and D. N. Brindley. 1990. Stimulation of apolipoprotein secretion in very-low-density and high-density lipoproteins from cultured rat hepatocytes by dexamethasone. *Biochem. J.* **271**: 575–583.
  34. Sparks, J. D., and C. E. Sparks. 1990. Insulin modulation of hepatic synthesis and secretion of apolipoprotein B by rat hepatocytes. *J. Biol. Chem.* **265**: 8854–8862.
  35. Wang, C. N., R. S. McLeod, Z. Yao, and D. N. Brindley. 1995. Effects of dexamethasone on the synthesis, degradation, and secretion of apolipoprotein B in cultured rat hepatocytes. *Arterioscler. Thromb. Vasc. Biol.* **15**: 1481–1491.
  36. Tanaka, M., H. Jingami, H. Otani, M. Cho, Y. Ueda, H. Arai, Y. Nagano, T. Doi, M. Yokode, and T. Kita. 1993. Regulation of apolipoprotein B production and secretion in response to the change of intracellular cholesteryl ester contents in rabbit hepatocytes. *J. Biol. Chem.* **268**: 12713–12718.
  37. Cartwright, I. J., and J. A. Higgins. 1996. Intracellular degradation in the regulation of secretion of apolipoprotein B-100 by rabbit hepatocytes. *Biochem. J.* **314**: 977–984.
  38. Sakata, N., X. Wu, J. L. Dixon, and H. N. Ginsberg. 1993. Proteolysis and lipid-facilitated translocation are distinct but competitive processes that regulate secretion of apolipoprotein B in HepG2 cells. *J. Biol. Chem.* **268**: 22967–22970.
  39. Thrift, R. N., J. Drisko, S. Dueland, J. D. Trawick, and R. A. Davis. 1992. Translocation of apolipoprotein B across the endoplasmic reticulum is blocked in a nonhepatic cell line. *Proc. Natl. Acad. Sci. USA.* **89**: 9161–9165.
  40. Yeung, S. J., S. H. Chen, and L. Chan. 1996. Ubiquitin-proteasome pathway mediates intracellular degradation of apolipoprotein B. *Biochemistry.* **35**: 13843–13848.
  41. Fisher, E. A., M. Zhou, D. M. Mitchell, X. Wu, S. Omura, H. Wang, A. L. Goldberg, and H. N. Ginsberg. 1997. The degradation of apolipoprotein B100 is mediated by the ubiquitin-proteasome pathway and involves heat shock protein 70. *J. Biol. Chem.* **272**: 20427–20434.
  42. Chen, Y., F. Le Caherec, and S. L. Chuck. 1998. Calnexin and other factors that alter translocation affect the rapid binding of ubiquitin to apoB in the Sec61 complex. *J. Biol. Chem.* **273**: 11887–11894.
  43. Benoist, F., and T. Grand-Perret. 1997. Co-translational degradation of apolipoprotein B-100 by the proteasome is prevented by microsomal triglyceride transfer protein. Synchronized translation studies on HepG2 cells treated with an inhibitor of microsomal triglyceride transfer protein. *J. Biol. Chem.* **272**: 20435–20442.
  44. Yao, Z., K. Tran, and R. S. McLeod. 1997. Intracellular degradation of newly synthesized apolipoprotein B. *J. Lipid Res.* **38**: 1937–1953.
  45. Yeung, S-C. J., and L. Chan. 1998. Hepatic apolipoprotein B biogenesis: an update. *Trends Cardiovasc. Med.* **8**: 8–14.
  46. Van Harken, D. R., C. W. Dixon, and M. Heimberg. 1969. Hepatic lipid metabolism in experimental diabetes. V. The effect of concentration of oleate on metabolism of triglycerides and on ketogenesis. *J. Biol. Chem.* **244**: 2278–2285.
  47. Miller, L. L. 1973. *Isolated Liver Perfusion and Its Applications*. Raven Press, New York. 11–52.
  48. Boren, J., M. Wettsten, A. Sjoberg, T. Thorlin, G. Bondjers, O. Wiklund, and S. O. Olofsson. 1990. The assembly and secretion of apoB-100-containing lipoproteins in HepG2 cells. Evidence for different sites for protein synthesis and lipoprotein assembly. *J. Biol. Chem.* **265**: 10556–10564.
  49. Bostrom, K., M. Wettsten, J. Boren, G. Bondjers, O. Wiklund, and



- S. O. Olofsson. 1986. Pulse-chase studies of the synthesis and intracellular transport of apolipoprotein B-100 in HepG2 cells. *J. Biol. Chem.* **261**: 13800–13806.
50. Bostrom, K., J. Boren, M. Wettsten, A. Sjoberg, G. Bondjers, O. Wiklund, P. Carlsson, and S. O. Olofsson. 1988. Studies on the assembly of apoB-100-containing lipoproteins in HepG2 cells. *J. Biol. Chem.* **263**: 4434–4442.
51. Cavallo, D., R. S. McLeod, D. Rudy, A. Aiton, Z. Yao, and K. Adeli. 1998. Intracellular translocation and stability of apolipoprotein B are inversely proportional to the length of the nascent polypeptide. *J. Biol. Chem.* **273**: 33397–33405.
52. Laemmli, U. K. 1970. Cleavage of structural proteins during the assembly of the head of bacteriophage T4. *Nature.* **227**: 680–685.
53. Sallach, S. M., and K. Adeli. 1995. Intracellular degradation of apolipoprotein B generates an N-terminal 70 kDa fragment in the endoplasmic reticulum. *Biochim. Biophys. Acta.* **1265**: 29–32.
54. Boren, J., S. Rustaeus, and S. O. Olofsson. 1994. Studies on the assembly of apolipoprotein B-100- and B-48-containing very low density lipoproteins in McA-RH7777 cells. *J. Biol. Chem.* **269**: 25879–25888.
55. Bamberger, M. J., and M. D. Lane. 1988. Assembly of very low density lipoprotein in the hepatocyte. Differential transport of apoproteins through the secretory pathway. *J. Biol. Chem.* **263**: 11868–11878.
56. Rustaeus, S., P. Stillemark, K. Lindberg, D. Gordon, and S. O. Olofsson. 1998. The microsomal triglyceride transfer protein catalyzes the post-translational assembly of apolipoprotein B-100 very low density lipoprotein in McA-RH7777 cells. *J. Biol. Chem.* **273**: 5196–5203.
57. Davis, R. A., A. B. Prewett, D. C. Chan, J. J. Thompson, R. A. Borchart, and W. R. Gallaher. 1989. Intrahepatic assembly of very low density lipoproteins: immunologic characterization of apolipoprotein B in lipoproteins and hepatic membrane fractions and its intracellular distribution. *J. Lipid. Res.* **30**: 1185–1196.
58. Cartwright, I. J., A. M. Hebbachi, and J. A. Higgins. 1993. Transit and sorting of apolipoprotein B within the endoplasmic reticulum and Golgi compartments of isolated hepatocytes from normal and orotic acid-fed rats. *J. Biol. Chem.* **268**: 20937–20952.
59. Cartwright, I. J., and J. A. Higgins. 1995. Intracellular events in the assembly of very-low-density-lipoprotein lipids with apolipoprotein B in isolated rabbit hepatocytes. *Biochem. J.* **310**: 897–907.
60. Cavallo, D., D. Rudy, A. Aiton, and K. Adeli. 1999. Studies on the degradative mechanisms regulating the posttranslational fragmentation of apolipoprotein B and the generation of the 70 kDa fragment. *J. Biol. Chem.* **274**: 23135–23143.
61. Sparks, J. D., and C. E. Sparks. 1994. Insulin regulation of triacylglycerol-rich lipoprotein synthesis and secretion. *Biochim. Biophys. Acta.* **1215**: 9–32.
62. Wang, H., X. Chen, and E. A. Fisher. 1993. N-3 fatty acids stimulate intracellular degradation of apoprotein B in rat hepatocytes. *J. Clin. Invest.* **91**: 1380–1389.
63. Fast, D. G., and D. E. Vance. 1995. Nascent VLDL phospholipid composition is altered when phosphatidylcholine biosynthesis is inhibited: evidence for a novel mechanism that regulates VLDL secretion. *Biochim. Biophys. Acta.* **1258**: 159–168.
64. Kendrick, J. S., and J. A. Higgins. 1999. Dietary fish oils inhibit early events in the assembly of very low density lipoproteins and target apoB for degradation within the rough endoplasmic reticulum of hamster hepatocytes. *J. Lipid Res.* **40**: 504–514.
65. Wang, Y., K. Tran, and Z. Yao. 1999. The activity of microsomal triglyceride transfer protein is essential for accumulation of triglyceride within microsomes in McA-RH7777 cells. *J. Biol. Chem.* **274**: 27793–27800.
66. Swift, L. L. 1995. Assembly of very low density lipoproteins in rat liver: a study of nascent particles recovered from the rough endoplasmic reticulum. *J. Lipid Res.* **36**: 395–406.
67. Arbeeny, C. M., D. S. Meyers, K. E. Bergquist, and R. E. Gregg. 1992. Inhibition of fatty acid synthesis decreases very low density lipoprotein secretion in the hamster. *J. Lipid Res.* **33**: 843–851.
68. White, A. L., D. L. Graham, J. LeGros, R. J. Pease, and J. Scott. 1992. Oleate-mediated stimulation of apolipoprotein B secretion from rat hepatoma cells. A function of the ability of apolipoprotein B to direct lipoprotein assembly and escape presecretory degradation. *J. Biol. Chem.* **267**: 15657–15664.
69. Sparks, J. D., H. L. Collins, I. Sabio, M. P. Sowden, H. C. Smith, J. Cianci, and C. E. Sparks. 1997. Effects of fatty acids on apolipoprotein B secretion by McArdle RH-7777 rat hepatoma cells. *Biochim. Biophys. Acta.* **1347**: 51–61.
70. Davis, R. A., and J. R. Boogaerts. 1982. Intrahepatic assembly of very low density lipoproteins. Effect of fatty acids on triacylglycerol and apolipoprotein synthesis. *J. Biol. Chem.* **257**: 10908–10913.
71. Patsch, W., T. Tamai, and G. Schonfeld. 1983. Effect of fatty acids on lipid and apoprotein secretion and association in hepatocyte cultures. *J. Clin. Invest.* **72**: 371–378.
72. Lin, Y., M. J. Smit, R. Havinga, H. J. Verkade, R. J. Vonk, and F. Kuipers. 1995. Differential effects of eicosapentaenoic acid on glycerolipid and apolipoprotein B metabolism in primary human hepatocytes compared to HepG2 cells and primary rat hepatocytes. *Biochim. Biophys. Acta.* **1256**: 88–96.
73. Salter, A. M., D. Wiggins, V. A. Sessions, and G. F. Gibbons. 1998. The intracellular triacylglycerol/fatty acid cycle: a comparison of its activity in hepatocytes which secrete exclusively apolipoprotein (apo) B100 very-low-density lipoprotein (VLDL) and in those which secrete predominantly apoB48 VLDL. *Biochem. J.* **32**: 667–672.